ELSEVIER

Chemical Geology 206 (2004) 231–248

CHEMICAL GEOLOGY
INCLUDING
ISOTOPE GEOSCIENCE

www.elsevier.com/locate/chemgeo

Chemostratigraphy of the Posidonia Black Shale, SW-Germany II. Assessment of extent and persistence of photic-zone anoxia using aryl isoprenoid distributions

L. Schwark[a,*], A. Frimmel[b]

[a] *Geological Institute, Cologne University, Zuelpicher Str. 49a, D-50674 Cologne, Germany*
[b] *Institut und Museum für Geologie und Paläontologie, Sigwartstr. 10, 72076 Tübingen, Germany*

Abstract

Aquatic depositional environments where anoxic conditions extend from bottom waters into the photic zone occurred frequently during the geologic past. Periods of photic-zone anoxia (PZA) can be recognized by the presence of specific lipids produced exclusively by the green sulphur bacteria (Chlorobiaceae) that are preserved in the sedimentary record. Chlorobiaceae perform anoxygenic photosynthesis that requires light penetration into H_2S-saturated waters. Sediment samples integrate paleoenvironmental conditions over time intervals ranging from, at best, a few decades to more commonly several millennia. Photic-zone anoxia recognized in paleoenvironmental analyses is thus defined as episodic, with no further interpretation on the duration and persistence of the anoxic events.

We provide here a high-resolution, multiproxy chemostratigraphy study for the Toarcian Posidonia Black Shale from the Dotternhausen section in SW-Germany, in order to assess duration and seasonal fluctuation of photic-zone anoxia based on the relative abundance of derivatives of Chlorobiaceae lipids. We assess the variability in the degree and persistence of photic-zone anoxia using an aryl isoprenoid ratio (AIR) obtained by calculating the proportion of the short-chain C_{13-17} versus the intermediate-chain C_{18-22} aryl isoprenoids. Higher relative abundance of the short-chain analogues is interpreted as indicating more intensive aerobic degradation of aryl isoprenoids. AIR varies between values of 0.5, indicative of persistent PZA phases, and 3.0 for short-termed episodic PZA events. Absolute concentration of aryl isoprenoids is negatively correlated with the AIR, which is in agreement with a progressive diagenetic breakdown of aryl isoprenoids. The AIR decreases are validated using independent palecological and geochemical redox indicators for the Posidonia Shale in SW-Germany.

Keywords: Photic-zone anoxia; Aryl isoprenoids; AIR; Chemostratigraphy; Posidonia Shale

1. Introduction

Depositional environments with permanent anoxic conditions that reach from the bottom into the surface waters are scarce in modern oceans. They are restricted to isolated basins including the Cariaco Trench and the Black Sea and to deep fjord environments like the Saanich Inlet in Vancouver Island. In environments where the anoxic zone extends from the sediment into the photic zone, conditions are suitable for the existence of green sulphur bacteria, the Chlorobiaceae. These organisms perform anoxygenic photosynthesis,

* Corresponding author. Tel.: +49-221470-2542; fax: +49-221470-5149.
E-mail address: lorenz.schwark@uni-koeln.de (L. Schwark).

0009-2541/$ - see front matter © 2004 Elsevier B.V. All rights reserved.
doi:10.1016/j.chemgeo.2003.12.008

thus requiring light penetration into H_2S-saturated waters.

Periods of photic-zone anoxia (PZA) can be recognized when specific lipids produced exclusively by the Chlorobiaceae are preserved in the sedimentary record. Such compounds derive from specifically adapted photosynthetic and accessory pigments, i.e., from bacteriochlorophylls and carotenoids. Chlorobiaceae utilize bacteriochlorophyll, which can be recognized in sediments and oils either directly or by the presence of its diagenetic breakdown products, the maleimides or alkylated pyrrol diones (Grice et al., 1996a; Pancost et al., 2002). Among the accessory pigments the Chlorobiaceae biosynthesize, diaromatic carotenoids of the isorenieratene-type (Liaaen-Jensen, 1978) show a distinctive $\delta^{13}C$-isotopic enrichment (Sirevåg et al., 1977). Whereas functionalized carotenoids are degraded rapidly in sediments (Baker and Louda, 1986), diaromatic carotenoids are geologically stable (Schaefle et al., 1977; Summons and Powell, 1986) and possess a high-preservation potential. Aromatic carotenoids undergo diagenetic transformation that can result in cleavage of the isoprenoid chain to form aryl isoprenoids. These compounds exist in the C_{10}–C_{31} range (Ostroukhov et al., 1982; Summons and Powell, 1986, 1987; Requejo et al., 1992). Successive reduction of the aryl isoprenoid chain length directly affects free aryl isoprenoid molecules (Summons and Powell, 1987; Schwark and Püttmann, 1990; Yu et al., 1990; Hartgers et al., 1994). Furthermore, side-chain cleavage was also suggested to occur with covalently bound and sulfur-sequestered aryl isoprenoid moieties in (proto)kerogens (Hartgers et al., 1994; Koopmans et al., 1996). In addition to the cleavage of the isoprenoid chain, diaromatic carotenoids may undergo cyclisation reactions. These are known to occur with regular carotenoids (Byers and Erdman, 1981; Achari et al., 1973) but have been demonstrated to occur most frequently with diaromatic carotenoids leading to a variety of contracted multiaromatic carotenoids (Grice et al., 1996b; Koopmans et al., 1996; Sinninghe Damsté et al., 2001). Posidonia Shale sediments in Dotternhausen, SW-Germany, do not contain significant amounts of contracted multiaromatic carotenoid derivatives (van Kaam-Peters, 1997).

When aryl isoprenoids are used in paleoenvironemental reconstructions, it is necessary to demonstrate that they are derived from isorenieratene precursors and thus, from Chlorobiaceae, because other sources of aryl isoprenoids, e.g., β- and γ-carotene, also exist in sedimentary environments (Hartgers et al., 1994; Koopmans et al., 1996, 1997). The origin of aryl isoprenoids from Chlorobiaceae can be confirmed by their relatively enriched $\delta^{13}C$-signatures (Hartgers et al., 1994; Grice et al., 1996b; Koopmans et al., 1996). For the Dotternhausen section, the $\delta^{13}C$-signatures of aryl isoprenoid clearly demonstrate an origin from Chlorobiaceae-derived isorenieratene (Schouten et al., 2000).

In this investigation of the Posidonia Black Shale from Dotternhausen, we assess the potential to relate systematic variations in aryl isoprenoid concentrations and their relative distribution to syndepositional changes in the water-column redox system. We interpret such changes in terms of the persistence and seasonal fluctuations in photic-zone anoxia (PZA) in the shallow shelf sea of the Toarcian Tethys. PZA fluctuations in the Posidonia Shale of the study area will be discussed in relation to an existing palecological (Seilacher, 1982; Kaufmann, 1978; Riegraf, 1985; Röhl et al., 2001; Schmid-Röhl et al., 2002) and geochemical (Küspert, 1982; Moldowan et al., 1986; van Kaam-Peters, 1997; Schouten et al., 2000; Schmid-Röhl et al., 2002; Frimmel et al., 2004) framework. For a detailed description of paleoenvironmental conditions prevailing during deposition of the Posidonia Shale, we refer to those publications and references therein.

2. Geological framework

A detailed summary of the geology of the study area is given in Röhl et al. (2001), Schmid-Röhl et al. (2002), and Röhl and Schmid-Röhl (2004). Here, we provide a short summary with specific emphasis on the role of sea-level variation and interpretation of sedimentological and palecological features in a sequence stratigraphic framework. The Mesozoic is characterized by a continent constellation where, at the beginning, Gondwana and Laurussia are combined in the Pangaea supercontinent, which starts to break up during the Late Triassic with the opening of the Proto-Atlantic during the Cretaceous. During the Lower Jurassic, present-day Europe was located on the broad and extensive Laurussian continental shelf that

opened towards the southeast into the deep Tethyan Ocean (Ziegler, 1988). This shallow shelf area contained various islands of variable size (Fig. 1), submarine sills, and deeper subbasins. All of these topographical features contributed to (episodic) restriction of water circulation across the shallow shelf sea, especially during periods of sea-level lowstand. The Lower Toarcian is characterized by an extensive transgressive phase, associated with the breakup of Pangaea (Haq et al., 1988; Hallam, 2001). This transgression established the initial marine connection between the northern Arctic part of the Panthalassa Ocean and the equatorial Tethys Ocean. This marine corridor enabled the exchange of northern Panthalassian cold waters and warm, saline Tethyan waters on the shelf areas, a setting similar to that of the Western Interior Seaway during the Cretaceous. During the Lower Toarcian, the study area was located at a paleolatitude between 30° and 40° on the Northern Hemisphere, thus subject to an intensive monsoonal-driven climate system (Parrish, 1993; Röhl et al., 2001) with predominantly warm and humid conditions. The study area in SW-Germany (Fig. 1) was connected to other shelf subbasins with bituminous black shale deposition: these were the Paris basin towards the west and the North Sea and Yorkshire basins to the north, the latter two linked via the NW-German basin. Separation of the continuous North Sea, Yorkshire, and NW-German basin from the southerly Paris and SW-German basins was provided by the east–west trending landmasses of the London Brabant, the Rhenish, and the Bohemian Massifs (Fig. 1).

The stratigraphic and palecological evolution of the Posidonia Shale in the study area of Dotternhausen is summarized in Fig. 2. The beginning of the Lower Toarcian or Lias ε is defined biostratigraphically by the disappearance of the *Pleuroceras* and first occurrence of the *Dactylioceras* ammonite groups. The Lower Toarcian consists of three ammonite zones, namely, the *tenuicostatum*, *falciferum*, and *bifrons* zones and a number of ammonite subzones (Fig. 2), of which, the *exaratum* subzone is of special importance, because of its coincidence with a pronounced negative carbon-isotope excursion. The topmost part of the Lias δ or Pliensbachian is composed of the so-called *spinatum* bank, a fully marine platform carbonate deposited under oxygenated shallow-water conditions. The lithological subdivision of the Lower Toarcian succession in SW-Germany derives from 19th century quarry workers (Fig. 2) and starts with the so-called "Blaugraue" and "Aschgraue Mergel", which consist of

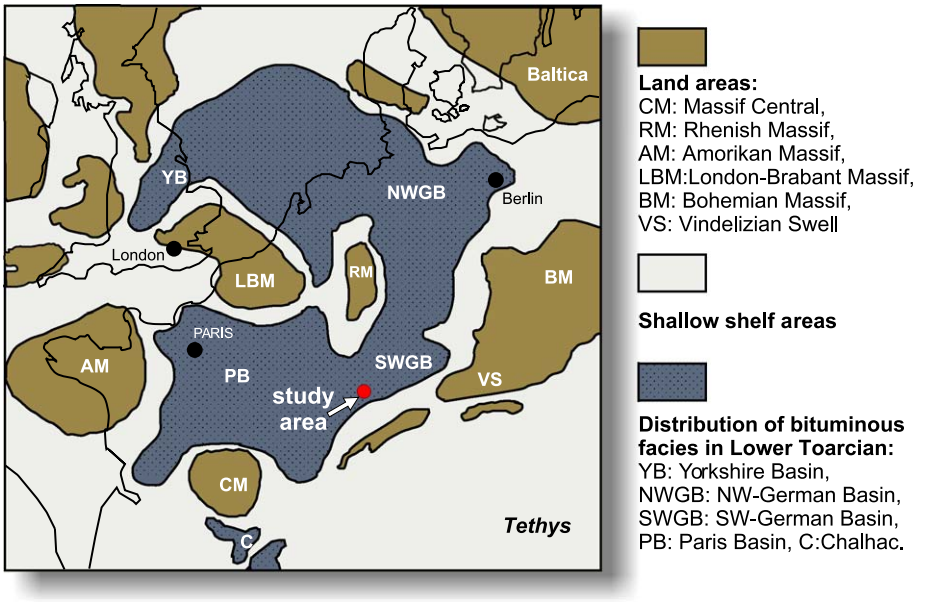

Fig. 1. Simplified paleogeograhic map of Liassic continental shelf area between Baltica and Laurentia after Ziegler (1982) with location of study area.

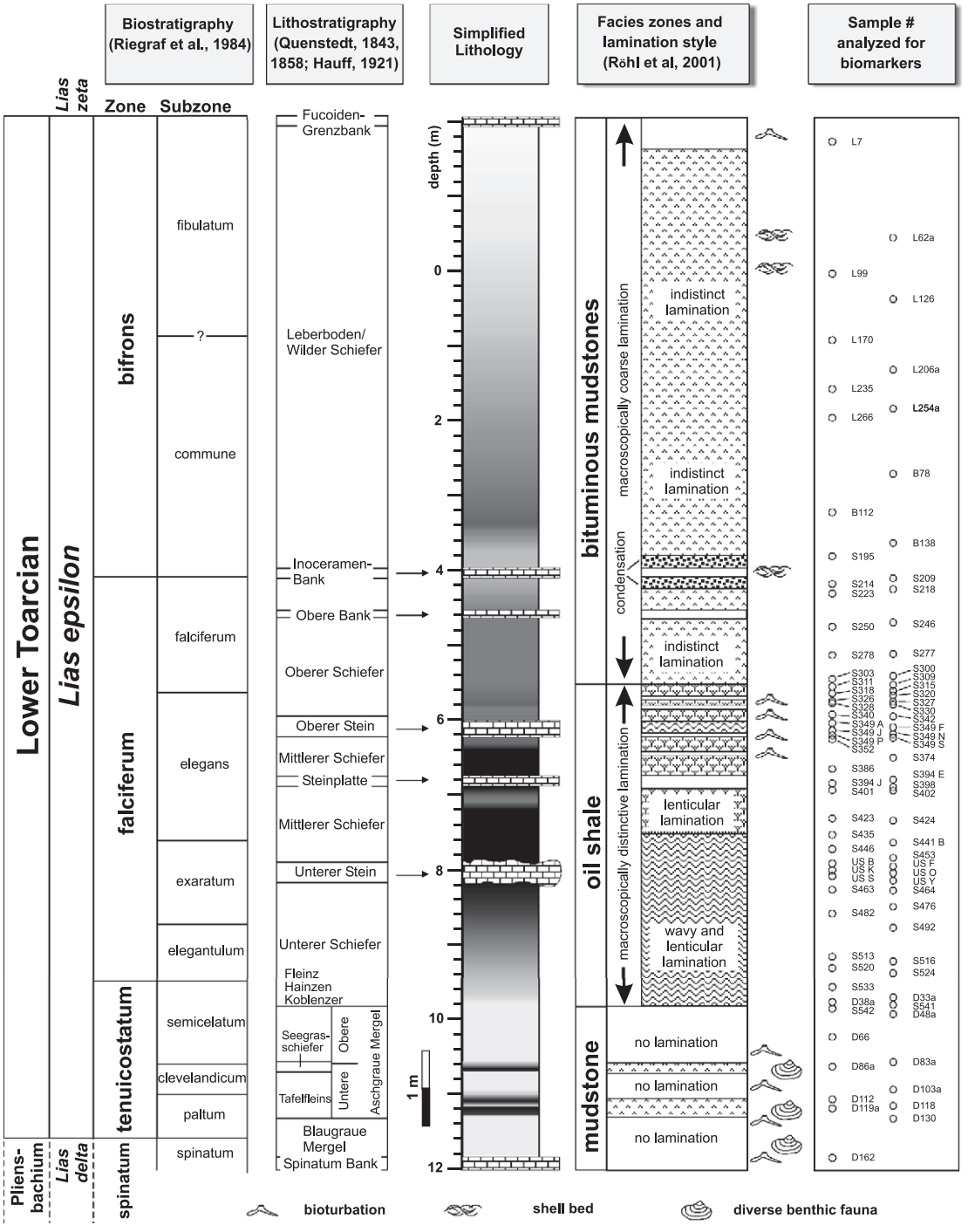

Fig. 2. Stratigraphic section of the Posidonia Shale in Dotternhausen, SW-Germany. Ammonite biostratigraphy follows Riegraf (1985). Local German names for lithostratigraphic units are from Quenstedt (1843, 1858) and Hauff (1921). Facies zones and lamination style is based on the summary in Röhl et al. (2001) and references listed therein. Codes of samples subjected to geochemical analysis are identical to those used in Table 1.

Table 1
Sample list including basic sedimentological and palecological parameters

Sample code	Depth (cm) to datum	Ammonite subzone	Lamination type	Faunal content	Sequence stratigraphic label	Sequence stratigraphic position
L7	− 172.4	fibulatum	no lamination	BB	○	HST
L62a	− 44.3	fibulatum	indistinct	Pd	○	HST
L99	3.5	fibulatum	indistinct	Bb	○	HST
L126	37.5	fibulatum	indistinct	Bb	○	HST
L170	92.2	commune	indistinct	Bb	○	HST
L206a	131.9	commune	indistinct	Bb	○	HST
L235	157.4	commune	indistinct	nbf	○	HST
L254a	183.5	commune	indistinct	Pdd	○	HST
L266	195.8	commune	indistinct	nbf	○	HST
B78	270.6	commune	indistinct	nbf	○	HST
B112	323.0	commune	indistinct	nbf	○	HST
B138	363.9	commune	indistinct	nbf	○	HST
S195	381.8	commune	indistinct	jm + Pd	♦	mfz
S209	411.0	falciferum	indistinct	Pd/Dp	♦	mfz
S214	418.6	falciferum	indistinct	Pd/Dp	♦	mfz
S218	425.7	falciferum	indistinct	Pd/Dp	♦	mfz
S223	431.3	falciferum	indistinct	pd	♦	mfz
S246	470.0	falciferum	indistinct	nbf	●	upper TST
S250	475.5	falciferum	indistinct	nbf	●	upper TST
S277	512.0	falciferum	distinctive	jm	●	upper TST
S278	513.5	falciferum	distinctive	jm	●	upper TST
S300	541.3	falciferum	distinctive	jm	●	upper TST
S303	545.4	falciferum	distinctive	jm	●	upper TST
S309	553.2	falciferum	distinctive	nbf	●	upper TST
S311	555.5	falciferum	lenticular	Bb	●	upper TST
S315	561.1	falciferum	lenticular	Bb	●	upper TST
S318	564.5	elegans	lenticular	Bb	●	upper TST
S320	567.0	elegans	lenticular	Bb	●	upper TST
S326	575.1	elegans	lenticular	Bb	●	upper TST
S327	575.8	elegans	lenticular	BB	●	upper TST
S328	577.6	elegans	lenticular	BB	●	upper TST
S330	579.5	elegans	lenticular	jm	●	upper TST
S340	592.6	elegans	lenticular	nbf	●	upper TST
S342	595.2	elegans	no lamination	BH	●	upper TST
S349 A	604.2	elegans	wavy and lenticular	nbf	●	upper TST
S349 F	609.5	elegans	wavy and lenticular	nbf	●	upper TST
S349 J	613.9	elegans	wavy and lenticular	nbf	●	upper TST
S349 N	618.8	elegans	wavy and lenticular	nbf	●	upper TST
S349 P	620.5	elegans	wavy and lenticular	nbf	●	upper TST
S349 S	623.5	elegans	wavy and lenticular	nbf	●	upper TST
S352	625.5	elegans	no lamination	BB	★	lower TST
S374	650.3	elegans	lenticular	jm	★	lower TST
S386	665.2	elegans	lenticular	nbf	★	lower TST
S386	665.2	elegans	lenticular	nbf	★	lower TST
S394 E	679.5	elegans	no lamination	nbf	★	lower TST
S394 J	684.5	elegans	no lamination	nbf	★	lower TST
S398	689.5	elegans	lenticular	nbf	★	lower TST
S401	693.5	elegans	lenticular	jm	★	lower TST
S402	694.3	elegans	lenticular	nbf	★	lower TST
S423	731.2	elegans	lenticular	nbf	★	lower TST
S424	734.1	elegans	wavy and lenticular	jm	★	lower TST

(continued on next page)

Table 1 (*continued*)

Sample code	Depth (cm) to datum	Ammonite subzone	Lamination type	Faunal content	Sequence stratigraphic label	Sequence stratigraphic position
S435	753.0	elegans	wavy and lenticular	jm	★	lower TST
S441 B	763.4	exaratum	wavy and lenticular	Ms	★	lower TST
S446	772.1	exaratum	wavy and lenticular	jm	★	lower TST
S453	783.7	exaratum	wavy and lenticular	nbf	★	lower TST
US B	791.1	exaratum	wavy and lenticular	nbf	☆	lower TST (Unterer Stein)
US F	795.1	exaratum	wavy and lenticular	nbf	☆	lower TST (Unterer Stein)
US K	800.1	exaratum	wavy and lenticular	nbf	☆	lower TST (Unterer Stein)
US O	804.1	exaratum	wavy and lenticular	nbf	☆	lower TST (Unterer Stein)
US S	808.1	exaratum	wavy and lenticular	nbf	☆	lower TST (Unterer Stein)
US Y	814.1	exaratum	wavy and lenticular	nbf	☆	lower TST (Unterer Stein)
S463	826.2	exaratum	wavy and lenticular	nbf	★	lower TST
S464	827.4	exaratum	wavy and lenticular	nbf	★	lower TST
S465	829.7	exaratum	wavy and lenticular	nbf	★	lower TST
S476	848.9	exaratum	wavy and lenticular	nbf	★	lower TST
S482	858.0	exaratum	wavy and lenticular	Pd	★	lower TST
S492	877.0	exaratum	wavy and lenticular	nbf	★	lower TST
S513	915.5	elegantulum	wavy and lenticular	Pd	★	lower TST
S516	921.9	elegantulum	wavy and lenticular	Pd	★	lower TST
S520	930.8	elegantulum	wavy and lenticular	nbf	★	lower TST
S524	937.7	elegantulum	wavy and lenticular	Pd	★	lower TST
S533	957	semicelatum	wavy and lenticular	Bb	★	lower TST
D33a	971.1	semicelatum	wavy and lenticular	Bb	★	lower TST
D38a	977.2	semicelatum	wavy and lenticular	Bb	★	lower TST
S541	981	semicelatum	wavy and lenticular	BB	★	lower TST
S542	986.1	semicelatum	wavy and lenticular	Bb	★	lower TST
D48a	993.5	semicelatum	no lamination	BB	★	lower TST
D66	1023.8	semicelatum	no lamination	BB	★	lower TST
D83a	1057	semicelatum	no lamination	BB	★	lower TST
D86a	1063	clevelandicum	indistinct	nbf	▲	LST
D103a	1093.6	clevelandicum	no lamination	BB	▲	LST
D112	1106.6	paltum	indistinct	nbf	▲	LST
D118	1115.3	paltum	indistinct	BB	▲	LST
D119a	1118.7	paltum	indistinct	nbf	▲	LST
D130	1132.3	paltum	no lamination	BB	○	HST
D162	1184.6	spinatum	no lamination	BB	○	HST

Abbreviations for faunal content: Pd = *Pseudomytiloides dubius* association, Dp = *Discina papyrecea* association, Bb = *Bositra buchi* association, Ms = *Meleagrinella substriata* association, Pd/Dd = *P. dubius*/*D. papyrecea* association, nbf = no benthic fauna, BB = bioturbation and benthic fauna, jm = juvenile mussels, BH = bioturbation horizons. Abbreviations used for sequence stratigraphic position: ○ HST, highstand systems tract; ♦ mfz, maximum flooding surface; ● TST, upper transgressive systems tract; ★ TST, lower transgressive systems tract; ☆ TST, lower transgressive systems tract (Unterer Stein); ▲ LST, TST, lower transgressive systems tract.

heavily bioturbated and macrobenthos-rich marly mudstones. Two black shale intervals, the lower "Tafelfleins" and the upper "Seegrasschiefer" horizons are intercalated into the marls of the *tenuicostatum* zone (Fig. 2). A gradational transition of the *tenuicostatum* marls and mudstones into the bituminous oil-shales of the *falciferum* zone is due to a rapid transgression and deepening of the basin. The oil shales of the *falciferum* zone grade into organic matter-rich black shales of the bifrons zone and are intercalated by five carbonate horizons. These are, from base to top, the "Unterer Stein", "Steinplatte", "Oberer Stein", "Obere Bank," and "Inoceramus Bank", as shown in Fig. 2.

The sequence stratigraphic framework consists of a sequence boundary between the uppermost Pliensbachian and the Lower Toarcian, with the *spinatum* bank representing the highstand systems tract (HST) of the lower sequence. A global transgression of second order is placed at the *falciferum/bifrons* transition (Hallam, 2001; de Graciansky et al., 1998) with

a superimposed third-order transgression/regression couplet indicating a major regressive phase in the tenuicostatum zone (Fig. 2). Sea level interpretations based on Haq et al. (1988) attribute a complete third-order cycle (Upper Absaroka B-4.3), being part of the second-order Upper Absaroka B-4 cycle, to the Lower Toarcian. Refinement of the sequence stratigraphic evolution of the study area in SW-Germany by Röhl and Schmid-Röhl (2004) and Röhl et al. (2001) indicates a forced regression in the lowermost *tenuicostatum* zone. Sea level reaches a minimum in the *clevelandicum* subzone (Fig. 2) with the lowstand systems tract (LST) persisting through the *paltum* and clevelandicum subzones. The transgressive phase starts in the lowermost *semicelatum* subzone and can be separated into a lower transgressive systems tract (TST) that commences in the Oberer Stein of the *elegans* subzone (Fig. 2) before passing into the upper transgressive systems tract (TST) that reaches up to the Inoceramus Bank at the *falciferum/bifrons*-transition. Here, the maximum flooding surface (mfz) is marked by two distinctive condensation horizons enclosing the Inoceramus Bank. Subsequently, the highstand systems tract (HST) of the *bifrons* zone represents the uppermost part of the studied sequence. For a detailed description of the sequence stratigraphic interpretation, see Röhl and Schmid-Röhl (2004) including their extensive literature compilation of measured sections. The sequence stratigraphic position of the samples used in this chemofacies study, as well as their lamination style and faunal content, is based on the work by Röhl and Schmid-Röhl (2004) and Röhl et al. (2001) and summarized in Table 1. Depositional models based on molecular geochemical and palecological interpretations in a sequence stratigraphic framework are discussed in Frimmel et al. (2004).

3. Methods and materials

Samples reported in this study are identical to those studied by Frimmel et al. (2004). Briefly, samples were collected in measured sections of the Posidonia Shale in a cement quarry in Dotternhausen, SW-Germany, described in detail in Riegraf (1985), Röhl et al. (2001), and Schmid-Röhl et al. (2002). Thickness of sampled sediment intervals was limited to 2–8 mm in order to minimize time-averaging effects. The up-section part of the Dotternhausen quarry is affected by minor weathering and thus, is not suitable for molecular geochemical analysis. In order to avoid any weathering artefacts, sample material for the upper part of the studied sequence, the *bifrons* zone, was obtained from fully cored research wells Laufen (BEB 1008) and Denkingen (BEB 1012). These sections are correlated perfectly with the Dotternhausen section, as described in Röhl et al. (2001) and Schmid-Röhl et al. (2002).

Extraction of soluble organic matter, its chromatographic separation into compound classes, and subsequent gas chromatography (GC-FID) and gas chromatography coupled to mass spectrometry (GC/MS) analysis was performed on ground and dried sediment samples as described in Schwark et al. (1998). Briefly, extracts were obtained by Accelerated Solvent Extraction (ASE) at 75 °C and 50 bars pressure with dichloromethane as the solvent. Compound class separation afforded medium pressure liquid chromatography (MPLC) as described by Radke et al. (1980) using an MKW-2 instrument. 1,1-Binaphthyl was added as an internal standard to the aromatic hydrocarbon fractions prior to GC/MS analysis.

GC/MS analysis was performed on an HP5890-II coupled to an HP5889 MS-engine. The GC was equipped with an HP5 column (50 m, 0.25 mm ID) coated with 5% chemically bonded phenyl–methyl–silicon (0.25 μm film thickness). Sample injection was achieved via an on-column injector. Helium was used as the carrier gas in constant flow mode at 0.5 ml/min. The GC oven temperature was programmed from 70 to 140 °C at a rate of 10 °C/min, followed by a second gradient from 140 to 320 °C at a rate of 3 °C/min. The mass spectrometer was operated at 70 eV in full scan-mode recording from $m/z = 50$ to $m/z = 600$. Data acquisition and processing was performed using an HP MS-ChemStation data system. Peak identification was carried out by comparison of mass spectra with those of the system library and by comparison with published spectra.

4. Results

For basic information on the abundance and type of organic matter determined by elemental analysis and

Rock Eval, refer to our detailed studies by Frimmel et al. (2004) and Schmid-Röhl et al. (2002). The amount of solvent-extractable organic matter varies between 100 and 13,500 ppm (Fig. 3, Table 2) with very low concentrations encountered for the Pliensbachian and the *tenuicostatum* zone. The three lower and very pure carbonate horizons also show very low extract yields, whereas the marly upper two carbonate horizons give intermediate extract yields. In general, the highest bitumen concentrations occur in the lower *falciferum* zone and then gradually decline towards the top of the *bifrons* zone. Most samples give TOC-normalized extract yields of 40–70 mg ext/gTOC with peak values of >100 mg ext/gTOC occurring for samples of the Unterer Stein and the Pliensbachian carbonate only (Fig. 3, Table 2). The samples from the *tenuicostatum* zone all reveal normalized extract yields around 50 mg ext/gTOC with no differentiation between the bioturbated mudstones and the two black shale intervals. The gradation of normalized extract yields at the onset of black shale deposition in the uppermost *semicelatum* subzone is much less pronounced than observed for

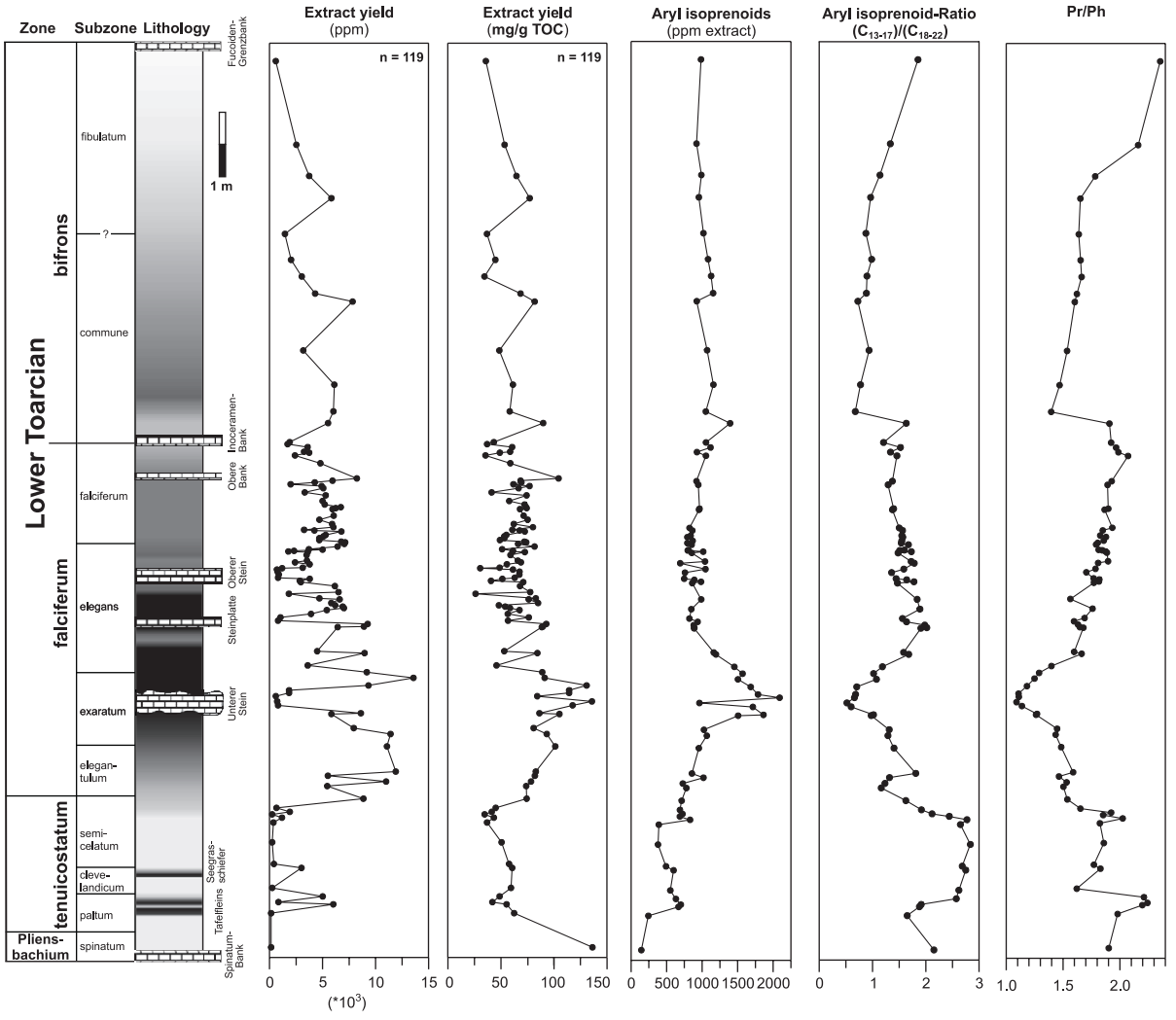

Fig. 3. Stratigraphic variation of total extract yields (ppm), TOC-normalized extract yields (mg/gTOC), abundance of aryl isoprenoids (ppm) and molecular redox parameters AIR and pr/ph ratio.

Table 2
Extract yields, concentrations of aryl isoprenoids and selected molecular redox and PZA indicators pr/ph ratio and AIR

sample code	depth (cm) to datum	Extract yield (ppm)	Extract yield (mg/gTOC)	Aryl isoprenoids (ppm)	Aryl isoprenoids (mg/gTOC)	AIR	pr/ph- ratio	seq. strat. label
L7	-172.4	590	36	984	35	1.85	2.35	❍
L62a	-44.3	2530	54	921	49	1.33	2.16	❍
L99	3.5	3740	65	990	64	1.14	1.78	❍
L126	37.5	5830	77	954	74	0.96	1.65	❍
L170	92.2	1450	37	1019	38	0.88	1.64	❍
L206a	131.9	2030	45	1084	49	0.98	1.65	❍
L235	157.4	3040	35	1126	39	0.9	1.66	❍
L254a	183.5	4300	69	1154	79	0.88	1.62	❍
L266	195.8	7830	82	925	76	0.72	1.60	❍
B78	270.6	3180	49	1070	52	0.93	1.54	❍
B112	323	6110	61	1159	71	0.77	1.47	❍
B138	363.9	6020	58	1052	61	0.68	1.40	❍
S195	381.8	5520	90	1394	125	1.63	1.91	◆
S209	411	1899	43	1054	46	1.21	1.92	◆
S214	418.6	3590	61	1118	68	1.52	1.97	◆
S218	425.7	3250	59	927	54	1.34	1.99	◆
S223	431.3	2396	36	1054	37	1.46	2.07	◆
S246	470	5939	69	921	63	1.37	1.93	●
S250	475.5	1990	62	946	58	1.29	1.89	●
S277	512	6240	74	964	72	1.4	1.90	●
S278	513.5	5940	68	956	65	1.37	1.87	●
S300	541.3	6022	80	822	66	1.5	1.93	●
S303	545.4	3257	61	862	52	1.56	1.85	●
S309	553.2	5288	55	839	46	1.55	1.83	●
S311	555.5	5080	53	792	42	1.57	1.88	●
S315	561.1	4690	49	867	43	1.55	1.86	●
S318	564.5	7129	74	792	59	1.54	1.80	●
S320	567	7050	66	853	56	1.67	1.79	●
S326	575.1	3710	51	807	41	1.6	1.81	●
S327	575.8	5000	172	798	137	1.51	1.85	●
S328	577.6	2313	62	1015	62	1.73	1.87	●
S330	579.5	3600	73	855	62	1.48	1.89	●
S340	592.6	3529	66	1041	69	1.73	1.90	●
S342	595.2	2404	69	691	48	1.78	1.81	●
S349 A	604.2	1188	31	1047	32	1.59	1.79	●
S349 F	609.5	757	68	759	51	1.36	1.70	●
S349 N	618.8	807	63	747	47	1.44	1.77	●
S349 P	620.5	3790	51	889	46	1.64	1.82	●
S349 S	623.5	2856	41	984	40	1.78	1.82	●
S352	625.5	2951	71	861	61	1.47	1.77	●
S374	650.3	4703	83	988	82	1.84	1.56	ℙ
S386	665.2	7010	59	848	50	1.89	1.76	ℙ
S394 E	679.5	1030	76	821	63	1.56	1.69	ℙ
S394 J	684.5	800	57	937	53	1.64	1.60	ℙ
S398	689.5	9250	93	882	82	1.98	1.63	ℙ
S401	693.5	8902	90	891	80	2.02	1.65	ℙ

(continued on next page)

TOC contents or HI values (Frimmel et al., 2004). The average extract composition is approximately 25% aliphatic, 30% aromatic hydrocarbons, 40% resins, and 5% asphaltenes. In this paper, only the distribution of selected aromatic and aliphatic hydrocarbons will be discussed. For details on the aliphatic hydrocarbon distribution of this sample set, see Frimmel et al. (2004).

Table 2 (*continued*)

sample code	depth (cm) to datum	Extract yield (ppm)	Extract yield (mg/gTOC)	Aryl isoprenoids (ppm)	Aryl isoprenoids (mg/gTOC)	AIR	pr/ph- ratio	seq. strat. label
S402	694.3	6424	89	887	79	1.91	1.68	ℙ
S423	731.2	4490	53	1164	62	1.58	1.60	ℙ
S424	734.1	8960	84	1195	101	1.68	1.66	ℙ
S435	753	3600	46	1453	67	1.19	1.40	ℙ
S441 B	763.4	9170	89	1570	140	1.02	1.29	ℙ
S446	772.1	13570	91	1504	137	1.07	1.25	ℙ
S453	783.7	9330	131	1683	220	0.7	1.18	ℙ
US F	795.1	1842	114	1787	204	0.68	1.11	ℍ
US K	800.1	590	84	2091	176	0.66	1.11	ℍ
US S	808.1	720	136	962	131	0.52	1.09	ℍ
US Y	814.1	800	118	1714	202	0.6	1.14	ℍ
S463	826.2	8610	86	1863	161	1.02	1.27	ℙ
S464	827.4	5830	105	1507	159	0.97	1.26	ℙ
S465	829.7	11080	94	1424	134	0.92	1.29	ℙ
S476	848.9	7940	81	1025	83	1.31	1.45	ℙ
S482	858	11410	93	1066	99	1.29	1.44	ℙ
S492	877	11070	101	954	97	1.4	1.48	ℙ
S513	915.5	11900	83	857	71	1.81	1.59	ℙ
S516	921.9	5500	82	1019	84	1.32	1.46	ℙ
S520	930.8	10990	78	728	57	1.23	1.53	ℙ
S524	937.7	5440	74	778	58	1.16	1.50	ℙ
S533	957	8850	74	712	53	1.63	1.54	ℙ
D33a	971.1	650	45	688	31	1.92	1.65	ℙ
D38a	977.2	1910	41	724	30	2.12	1.92	ℙ
S541	981	250	35	686	24	2.44	1.85	ℙ
S542	986.1	1170	43	830	36	2.77	2.02	ℙ
D48a	993.5	370	37	391	14	2.65	1.82	ℙ
D66	1023.8	250	51	379	19	2.84	1.86	ℙ
D83a	1057	410	58	492	28	2.68	1.77	ℙ
D86a	1063	3010	61	599	36	2.75	1.83	♦
D103a	1093.6	250	60	553	33	2.62	1.62	♦
D112	1106.6	5010	49	630	31	2.57	2.21	♦
D118	1115.3	840	42	700	29	1.91	2.24	♦
D119a	1118.7	6010	55	667	37	1.88	2.20	♦
D130	1132.3	150	62	244	15	1.65	1.98	❍
D162	1184.6	150	136	145	19	2.15	1.90	❍

The aromatic hydrocarbons of the Posidonia Shale in Dotternhausen consist mainly of benzenes, naphthalenes, phenanthrenes, dibenzothiophenes, and their alkylated analogues. In addition, tetrahydroretene, mono- to triaromatic steroids, aromatic secohopanes, and benzohopanes are present. Representative total ion chromatograms (TIC) of aromatic hydrocarbon fractions are shown in Fig. 4. In analogy to the distribution of aliphatic biomarkers, the composition of aromatic biomarkers points towards an almost exclusively marine origin for the extractable organic matter. In extracts of the Posidonia Shale from Dotternhausen, a series of aryl isoprenoids occurs in amounts of 145–2091 ppm of extractable organic matter or 30–220 μg/gTOC. Such compounds have not been reported to occur in the NW-German Posidonia Shale (Littke et al., 1991) or in the time- and facies-equivalent Whitby Mudstone of Yorkshire (Sælen et al., 2000). In this study, we detected only trace amounts of intact diaromatic carotenoids that were previously reported for Posidonia Shale samples of SW-Germany (van Kaam-Peters, 1997; Schouten et al., 2000). This is probably due to our stratigraphic high-resolution sampling approach in which we did not prepare aromatic hydrocarbon subfractions enriched in aromatic carotenoids as done by van Kaam-Peters (1997).

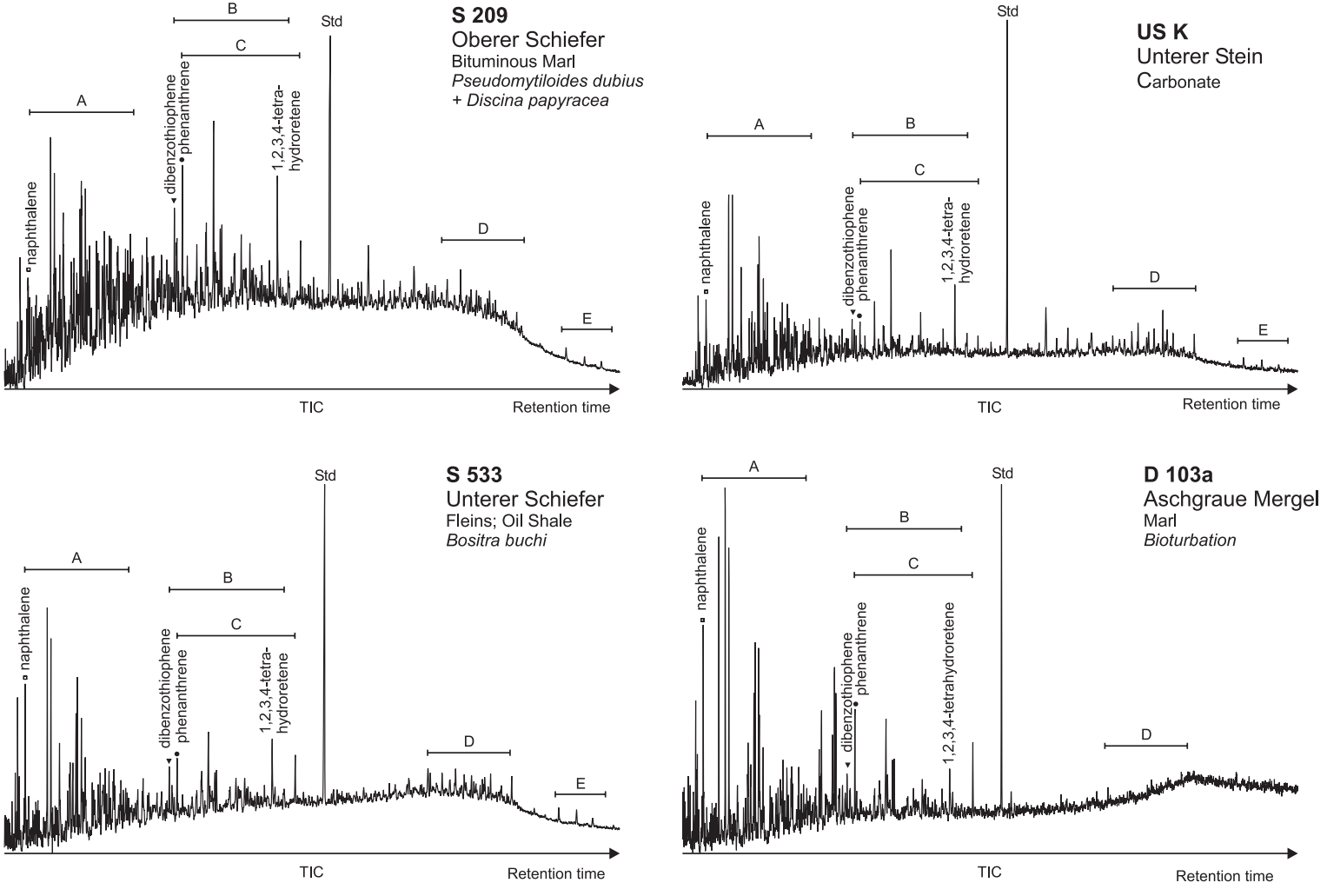

Fig. 4. Representative total ion chromatograms (TIC) for 4 samples showing the average gross composition of aromatic hydrocarbons. Bars indicate elution intervals of (A) = alkylated naphthalenes, (B) = alkylated dibenzothiophenes, (C) = alkylated phenanthrenes, (D) = mono- and trioaromatic steroids, (E) = benzohopanes; Std = 1,1-binaphthyl standard.

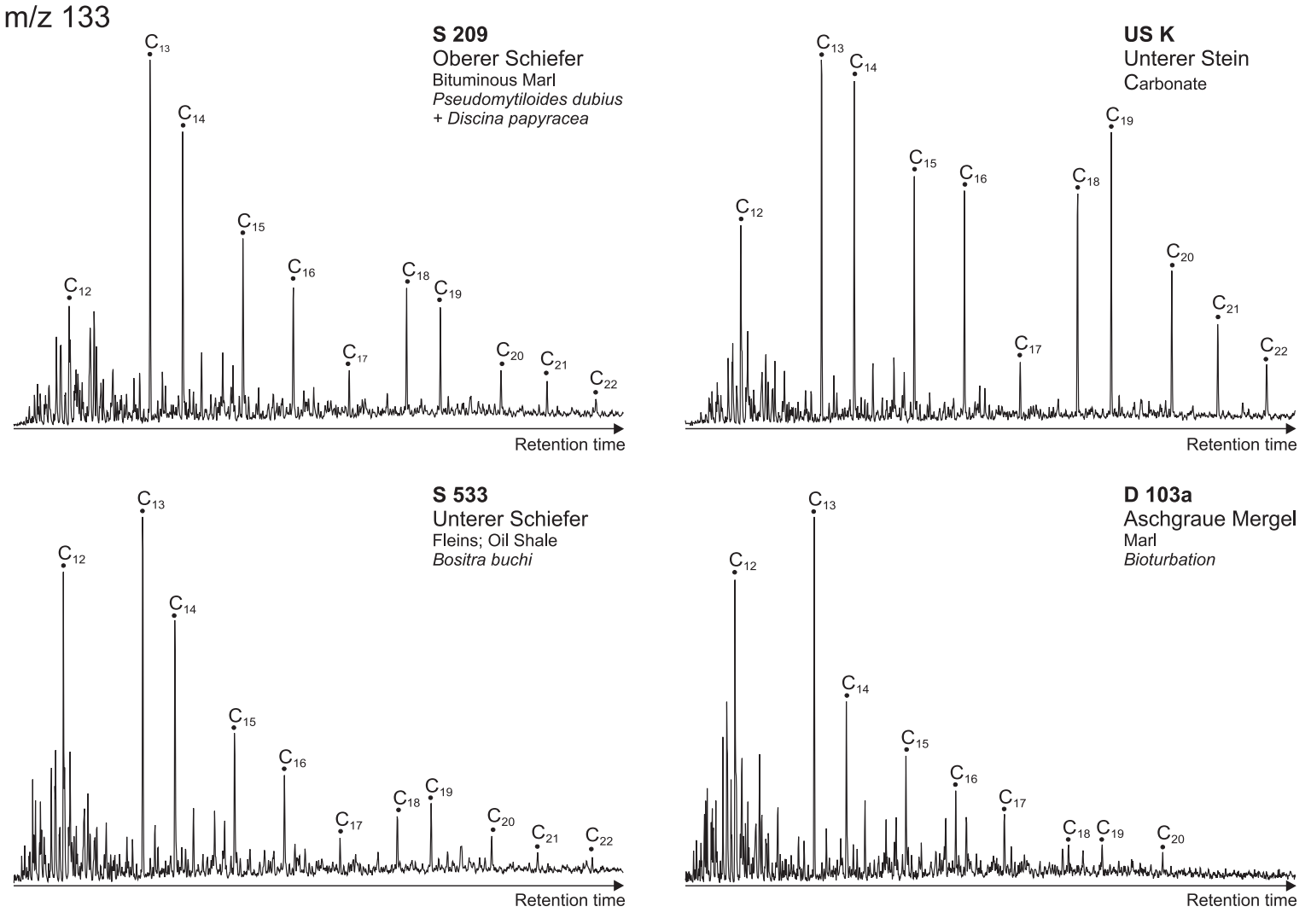

Fig. 5. Representative mass fragmentograms ($m/z = 133$) for four samples showing the average distribution and differences in chain length of aryl isoprenoid pseudohomologues.

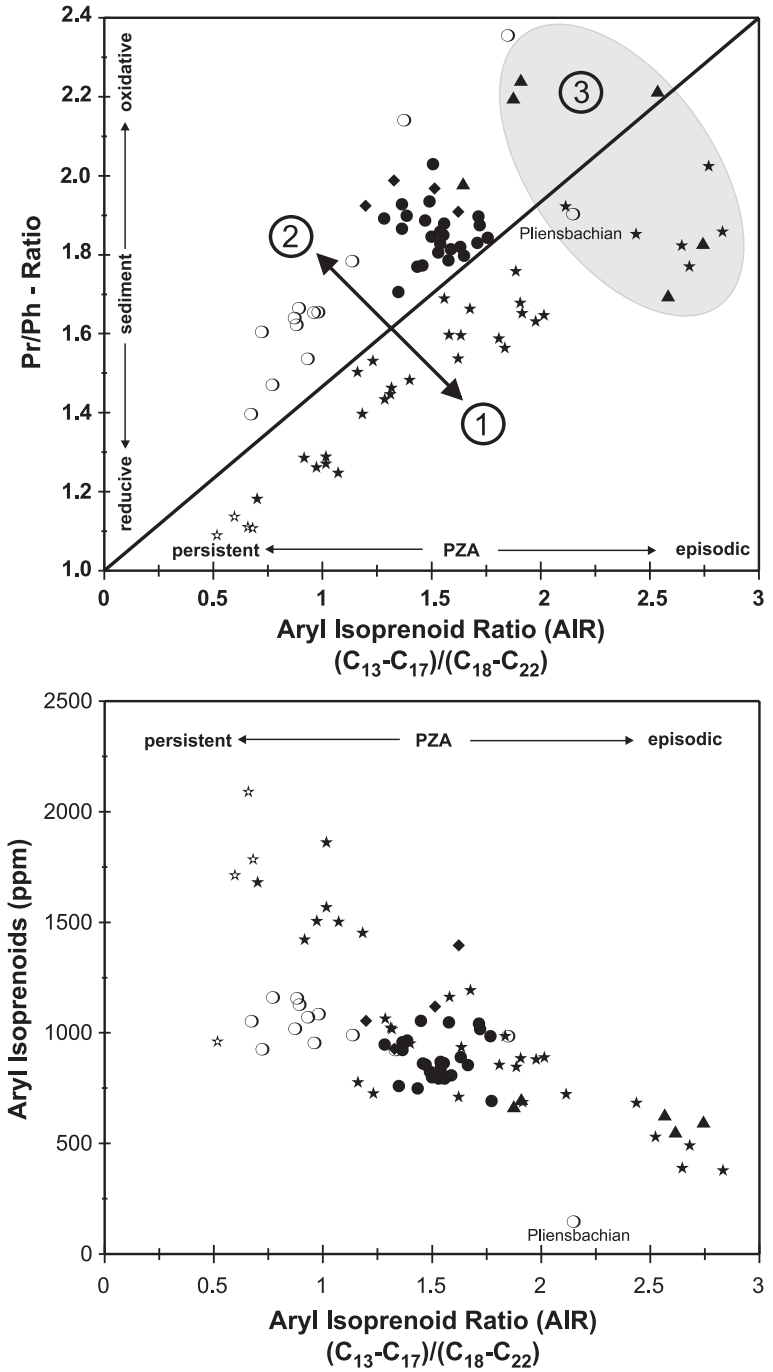

Fig. 6. Crossplot of aryl isoprenoid concentration (ppm) and molecular redox indicators pr/ph ratio against AIR. AIR increases with decreasing preservation of aryl isoprenoids. For AIRs versus pr/ph ratios, a differentiation into three groups is recognized. Group 1 contains the samples (★, ☆) from the lower TST deposited under intermediate sea level. Cluster 2 group samples (●, ◆, ○) deposited under high sea level prevailing under upper TST, mfz, and HST. Group 3 (▲) combines samples deposited under aerobic conditions during low sea level and intensive ventilation of shelf waters. Low AIR values indicate long-lived and permanent photic-zone anoxia (PZA) whereas high values indicate short-lived and episodic PZA.

The range of aryl isoprenoids detected in this study extends from C_{10} to C_{27}. Aryl isoprenoids in the C_{12}–C_{22} range are the most abundant and are present in all samples. Four representative aryl isoprenoid distributions are shown in Fig. 5 and the stratigraphic variation in total aryl isoprenoid concentrations is given in Fig. 3 and Table 2. Fig. 5 shows that the aryl isoprenoid distribution is highly variable throughout the section. Low molecular weight compounds dominate and higher molecular weight compounds are preferentially depleted in samples with low amounts of aryl isoprenoids (Table 2). The proportion of lower vs. higher molecular weight aryl isoprenoids was calculated using the ratio C_{13-17}/C_{18-22} and abbreviated as aryl isoprenoid ratio (AIR) as listed in Table 2. Over the Posidonia Shale profile, the concentrations of aryl isoprenoids and the AIR show a negative correlation (Figs. 3 and 6). Highest abundance of aryl isoprenoids occurs within the *exaratum* subzone, especially within the carbonate bank of the Unterer Stein. Aryl isoprenoid concentrations are particularly low in the mudstones of the *tenuicostatum* zone, except for two intercalated black shale horizons. A sharp increase in aryl isoprenoid concentrations occurs in the upper *semicelatum* subzone coinciding with the onset of black shale deposition. Throughout the *falciferum* and *bifrons* zones, the concentrations of aryl isoprenoids remain fairly constant except for the *exaratum* subzone mentioned above. The AIR starts with high values of 2.0 in the Pliensbachian and increases to stable values around 2.8 for the *tenuicostatum* zone, except for the lower black shale horizon (Fig. 3). Coinciding with the increase in aryl isoprenoid concentration, the AIR drops rapidly at the onset of black shale deposition in the uppermost *semicelatum* subzone (Fig. 3). Except for a distinctive minimum of 0.5 in the Unterer Stein, the AIR remains between values of 1 and 2 until reaching the mfz at the *falciferum*/*bifrons* zone transition. Within the condensation horizon of the mfz, the AIR approaches a minor maximum and then falls again to values <1 before recovering to average values of 2 in the *fibulatum* subzone.

5. Discussion

Aryl isoprenoids encountered in the Posidonia Shale of Dotternhausen show the Chlorobiaceae-indicative 2,3,6-methylation pattern. In combination with the $\delta^{13}C$ isotopic enrichment and the detection of intact diaromatic carotenoids of the isorenieratane-type (Schouten et al., 2000; van Kaam-Peters, 1997), this provides evidence that Chlorobiaceae are the biological source for aryl isoprenoids from the study site. The presence of Chlorobiaceae and the inferred episodes of PZA are in excellent agreement with previous descriptions of the chemofacies (Küspert, 1982; Moldowan et al., 1986; van Kaam-Peters, 1997; Schouten et al., 2000; Schmid-Röhl et al., 2002; Frimmel et al., 2004) and palecological (Seilacher, 1982; Kaufmann, 1978; Riegraf, 1985; Röhl et al., 2001; Schmid-Röhl et al., 2002) characterizations of the Posidonia Shale.

The variability in aryl isoprenoid distribution cannot be attributed to differences in thermal maturity over the 12 m of immature (Littke et al., 1991) Posidonia Shale succession because of a lack of secondary thermal sources, like hydrothermal fluids or magmatic dykes or sills that may affect organic matter maturity. Variable degrees of weathering or biodegradation that may affect biomarker distributions were not noted upon inspection of aliphatic and aromatic hydrocarbon distributions. Mineral–matrix effects related to clay and pyrite abundance or systematic dependencies on carbonate content were also excluded as factors controlling aryl isoprenoid composition because no systematic relationship with sulfur and carbonate content was observed. It must therefore be concluded that the variability in aryl isoprenoid composition is due to the primary environmental conditions during sedimentation and earliest diagenesis.

Variation in the concentrations of aryl isoprenoids may reflect initial productivity of Chlorobiaceae. Factors controlling Chlorobiaceae productivity may either be related to the extent to which the anoxic zone protruded into the photic zone or to the availability of essential nutrients. The total amount of Chlorobiaceae biomass incorporated in the sediment is then further governed by how long PZA persisted over a given time interval. Fig. 6 demonstrates the negative correlation between the degree of preservation of less degraded intermediate-chain aryl isoprenoids, measured by AIR, and the absolute concentrations of aryl isoprenoids. PZA persistence is controlled by the stability of water-column stratification, which in turn depends on water circulation on the shallow Toarcian

shelf. Depositional models for the Posidonia Shale assume a monsoonal-driven climate system (Röhl et al., 2001; Schmid-Röhl et al., 2002; Frimmel et al., 2004) leading to estuarine flow regimes during the summer and antiestuarine during the winter period. Continental freshwater surface run-off was high during summer monsoons but low during winter times when strong evaporation led to salinity enhancement in shelfal waters. It must thus be assumed that seasonal or quasi-seasonal (periods of years) destabilization of water stratification must have occurred during deposition of the Posidonia Shale.

Even with the small sampling intervals of 2–8 mm chosen for this study, an annual or subannual resolution of aryl isoprenoid distribution cannot be achieved. Each sample analyzed comprised approximately 10–500 years of deposition. The variability in aryl isoprenoid composition over the studied section, however, allows decadal periods of enhanced stability of water-column stratification to be assessed. This time-integrated and -averaged redox potential preserved in sediment samples based on aryl isoprenoid abundance and composition can be correlated with other available molecular redox indicators. For other molecular redox indicators determined on the same sample, identical restrictions with respect to time resolution and time integration apply.

The ratio of pristane versus phytane (pr/ph ratio) is a frequently applied molecular redox indicator (Peters and Moldowan, 1993). However, a number of factors not related to redox changes may influence the pr/ph ratio as discussed in ten Haven et al. (1988), Peters and Moldowan (1993), and Koopmans et al. (1999) complicating the interpretation of pr/ph ratios. The applicability of the ratio for determination of paleoredox conditions in the Posidonia Shale is discussed in detail in Frimmel et al. (2004). Although the absolute values of the pr/ph ratio produce questionable high redox potential values, the ratio does reflect the stratigraphic variability in the redox conditions in the Posidonia Shale sequence.

A crossplot of the pr/ph ratio and the AIR (Fig. 6) indicates a covariance between the two parameters whereby three groups of samples can be differentiated. The primary differentiation is between groups 1 and 2 (Fig. 6), both of which reveal a good individual correlation between AIR and pr/ph ratio. However, group 1 when compared with group 2 for a given AIR, gives pr/ph ratios consistently lower by approximately 0.5, or correspondingly for a given pr/ph ratio, AIR is consistently higher by approximately 1.5. This systematic offset must be related to differences in the degradation pathway of pristane and phytane versus aryl isoprenoid precursors, namely, phytol and isorenieratene. Group 3 contains samples derived from the lowermost LST and the HST sample from the Pliensbachian, which during sea level lowstand were partly affected by postdepositional subaerial exposure and oxidative degradation.

Our interpretation for the differential behavior of AIR values in groups 1 and 2 is based upon fluctuations of the chemocline caused by seasonal ventilation of the Toarcian shelf. Sluggish ventilation, due to restricted water exchange with the open Tethys Ocean, is linked to intermediate sea level (Frimmel et al., 2004) during the lower TST. High surface productivity and organic matter decomposition by sulfate-reducing bacteria in sediment and bottom waters during summer monsoons lead to an expansion of the euxinic zone, as represented by group 1, which contains all samples from the lower TST. After surface-flow inversion, that is, a shift to an antiestuarine flow pattern under dry winter conditions, the euxinic bottom waters were not completely flushed out of the basin. Therefore, Chlorobiaceae-derived lipids produced during the summer period were not exposed to aerobic degradation and longer-chain aryl isoprenoids were preserved. This scenario is best represented by samples from the *exaratum* subzone, whereas samples with high AIR in the lower TST group 1 predominantly derive from samples deposited prior to deposition of the *exaratum* subzone. At that time, sea level often was so low that, episodically, the euxinic bottoms waters generated through summer times were flushed out of the basin and oxidative degradation of aryl isoprenoids commenced during winter times.

Samples from group 2 for a given AIR show pr/ph ratios which are significantly higher than observed for group 1. Except for the LST samples from the basal regressive black shale of the *tenuicostatum* zone which belong to group 3, AIR values of samples plotting above the discrimination line between groups 1 and 2 do not exceed a value of 2.0. This indicates that aerobic degradation under low sea level and intensive basin ventilation did not occur. Samples from the mfz and the upper TST group together at higher AIR between 1.2 and 1.6, whereas most samples from the HST show a

much wider spread in AIR. However, most values are grouped in a cluster that shows considerably lower AIR when compared to the upper TST and mfz. The offset between the pr/ph ratio and AIR for groups 1 and 2 is related to the relative thickness of the euxinic versus oxygenated part of the water body. During sea-level highstand (>80 m) and improved ventilation, the water column was predominantly oxic and the thickness of the euxinic zone was only a few meters (<10 m). At intermediate sea level (~ 50 m) during the deposition of the lower TST, the thickness of the euxinic bottom-water layer increased to tens of meters (~ 10–30 m), and the remaining oxygenated surface water layer was of approximately equal thickness.

Algal primary production during the summer period is assumed to have been comparable for groups 1 and 2. For lower TST samples (group 1), very little aerobic degradation of algal-derived phytol proceeded during settling through a thinner oxygenated surface water layer. Organic detritus and fecal pellets of larger size and higher settling velocity (Röhl et al., 2001) passed rapidly through the oxygenated part of the stratified water body and suffered only minor degradation in the lower, euxinic zone.

Samples from group 2 show higher pr/ph ratios because phytol derived from surface-layer primary production settled through a much thicker oxygenated water body before reaching the euxinic zone. Thus, phytol was exposed much longer to aerobic degradation. Sediment starvation during mfz led to a decrease in mineral detritus and fecal pellets, which further decreased settling velocity for sinking particles (Röhl et al., 2001) and increased the exposure time to aerobic degradation. During deposition of the upper TST and mfz, the ratio of oxygenated versus euxinic water body was particularly high due to nutrient reduction in the distal part of the basin, significantly decreasing the settling times of particulate matter. During the HST preservation, conditions improved due to higher productivity and intensified stagnation.

Production of aryl isoprenoid precursors occurred exclusively within the euxinic zone due to the environmental demands of Chlorobiaceae. A direct dependency of Chlorobiaceae abundance on the thickness of the overlying oxygenated surface waters did not exist. This explains the differentiated response to redox conditions for phytol and isorenieratene during earliest diagenesis.

5.1. Depositional models

The evolution of bulk organic matter composition and biomarker composition in combination with sedimentological and palecological features allows a reconstruction of conditions leading to either black shale or mudstone deposition during the Toarcian as summarized in Frimmel et al. (2004) and Röhl et al. (2001). Sea-level change was identified as the major factor controlling overall chemofacies and the time-averaged redox potential. Here, we provide evidence based on different behaviors of compounds produced in the upper part of the euxinic zone and the upper part of the oxygenated surface waters in a stratified basin. Using phytol and its respective diagenetic products pristane and phytane, we monitored the early diagenetic fate of algal matter produced in oxygenated surface water. The fate of Chlorobiaceae-derived bacterial biomass produced in the upper part of the euxinic zone was followed by analysis of aryl isoprenoids.

During the lower TST, both ratios show a good correlation and a wide spread in time-averaged molecular redox indicators. During intermediate sea level of the lower TST, the redox boundary was positioned permanently high in the water column. Seasonal inversion of the flow regime on the shelf, from estuarine in summer to antiestuarine in winter, did not ventilate the entire basin and thus, near-bottom euxinic water masses were not flushed out regularly.

During high sea level as represented by upper TST, mfz, and HST, the water exchange with the Tethys Ocean was enhanced and the shelf areas became much better ventilated. An expansion of the euxinic zone and improved conditions for Chlorobiaceae were reached seasonally during summer. Photic-zone anoxia then deteriorated upon inversion of water currents and the switch to an antiestuarine flow pattern, which flushed out most of the previously built-up euxinic water masses.

The distribution of PZA-indicative diagenetic degradation products of isorenieratene, a compound produced by anoxygenic photosynthetic green sulfur bacteria, namely, the aryl isoprenoids, allows differentiation between PZA that prevailed seasonally and PZA that prevailed continuously over decades or longer.

Acknowledgements

Invitation by guest editors S. Rimmer and R. Schultz to present a part of these results at the GSA meeting in Denver 2002 (L.S.) is gratefully acknowledged. Sue Rimmer and two anonymous reviewers are thanked for helpful comments. We thank A. Schmid-Röhl and J. Röhl for interesting interdisciplinary cooperation and stimulating discussions on the depositional environment of the Posidonia Shale.

References

Achari, R.G., Shaw, G., Holleyhead, R., 1973. Identification of ionene and other carotenoid degradation products from the pyrolysis of sporopollenins derived from pollen exines. Chem. Geol. 12, 229–234.

Baker, E.W., Louda, J.W., 1986. Porphyrins in the geosphere. In: John, R.B. (Ed.), Biological Markers in the Sedimentary Record. Elsevier, Amsterdam, pp. 125–224.

Byers, J.D., Erdman, J.G., 1981. Low temperature degradation of carotenoids as a model for early diagenesis in recent sediments. In: Bjoroy, M. (Ed.), Advances in Organic Geochemistry 1981. Wiley, Chichester, pp. 725–735.

de Graciansky, P.C., Dardeau, G., Dommergues, J.L., Durlet, C., Marchand, D., Dumont, T., Hesselbo, S.P., Jacquin, T., Goggin, V., Meister, C., Mouterde, R., Rey, J., Vail, P.R., 1998. Ammonite biostratigraphic correlation and Early Jurassic sequence stratigraphy in France; comparisons with some U.K. sections. In: de Graciansky, P.-C., Hardenbol, J., Jacquin, T., Vail, P.R. (Eds.), Mesozoic and Cenozoic Sequence Stratigraphy of European Basins. S.E.P.M. Spec. Publ., vol. 60, pp. 583–622. Tulsa.

Frimmel, A., Oschmann, W., Schwark, L., 2004. Chemostratigraphy of the Posidonia Black Shale, SW-Germany: I. Influence of sea level variation on organic facies evolution. Chem. Geol. 206, 199–230 (this issue).

Grice, K., Gibbison, R., Atkinson, J.E., Schwark, L., Eckardt, C.B.E., Maxwell, J.R., 1996a. Maleimides (1H-pyrrole-2,5-diones) as indicators of anoxygenic photo-synthesis in ancient water columns. Geochim. Cosmochim. Acta 60, 3913–3924.

Grice, K., Schaeffer, P., Schwark, L., Maxwell, J.R., 1996b. Molecular indicators of palaeoenvironmental conditions in an immature Permian shale (Kupferschiefer, Lower Rhine Basin, North-West Germany) from free and S-bound lipids. Org. Geochem. 25, 131–147.

Hallam, A., 2001. A review of the broad pattern of Jurassic sea-level changes and their possible causes in the light of current knowledge. Palaeogeogr. Palaeoclimatol. Palaeoecol. 167, 23–37.

Haq, B.U., Hardenbol, J., Vail, P.R., 1988. Mesozoic and Cenozoic chronostratigraphy and cycles of sea-level change. In: Wilgus, C.K., Hastings, B.S., Posamentier, H., Wagoner, J.V., Ross, C.A., Kendall, C.G.S.C. (Eds.), Sea-Level Changes—An Integrated Approach. S.E.P.M. Spec. Publ., vol. 42, pp. 71–108. Tulsa.

Hartgers, W.A., Sinninghe Damsté, J.S., Requejo, A.G., Allan, J., Hayes, J.M., Ling, Y., Xie, T.-M., Primack, J., de Leeuw, J.W., 1994. A molecular and carbon isotopic study toward the origin and diagenetic fate of diaromatic carotenoids. In: Telnæs, N., van Graas, G., Øygard, K. (Eds.), Advances in Organic Geochemistry 1993. Org. Geochem., vol. 22. Elsevier Science Ltd, GB, pp. 703–725.

Hauff, B., 1921. Untersuchungen der Fossilfundstätte von Holzmaden im Posidonienschiefer des Oberen Lias Württembergs. Palaeontographica 64, 1–42.

Kaufmann, E.G., 1978. Benthic environments and paleoecology of the Posidonienschiefer (Toarcian). Neues Jahrbuch für Geologie und Paläontologie. Abhandlungen, Stuttgart 157, 18–36.

Koopmans, M.P., Köster, J., van Kaam-Peters, H.M.E., Kenig, F., Schouten, S., Hartgers, W.A., de Leeuw, J.W., Sinninghe Damsté, J.S., 1996. Diagenetic and catagenetic products of isorenieratene: molecular indicators for photic zone anoxia. Geochim. Cosmochim. Acta 60, 4467–4496.

Koopmans, M.P., de Leeuw, J.W., Sinninghe Damsté, J.S., 1997. Novel cyclised and aromatized diagenetic products of β-carotene in the Green River Shale. Org. Geochem. 26, 451–466.

Koopmans, M.P., Rijpstra, W.I.C., Klapwijk, M.M., de Leeuw, J.W., Lewan, M.D., Sinninghe Damsté, J.S., 1999. A thermal and chemical degradation approach to decipher pristane and phytane precursors in sedimentary organic matter. Org. Geochem. 30, 1089–1104.

Küspert, W., 1982. Environmental changes during oil-shale deposition as deduced from stable isotope ratios. In: Einsele, G., Seilacher, A. (Eds.), Cyclic and Event Stratification. Springer, Berlin, pp. 482–501.

Liaaen-Jensen, S., 1978. Marine carotenoids. In: Faulkner, D.J., Fenical, W.H. (Eds.), Marine Natural Products. Academic Press, New York, pp. 1–73.

Littke, R., Baker, D.R., Leythaeuser, D., Rullkoetter, J., 1991. Keys to the depositional history of the *Posidonia* Shale (Toarcian) in the Hils Syncline, Northern Germany. In: Tyson, R.V., Pearson, T.H. (Eds.), Modern and Ancient Continental Shelf Anoxia. Spec. Publ.-Geol. Soc. Lond., vol. 58, pp. 311–333.

Moldowan, J.M., Sundararaman, P., Schoell, M., 1986. Sensitivity of biomarker properties to depositional environment and/or source input in the Lower Toarcian of SW-Germany. Org. Geochem. 10, 915–926.

Ostroukhov, S.B., Arefyev, O.A., Makusina, V.M., Zabrodrina, M.N., Petrov, A.A., 1982. Monocyclic aromatic hydrocarbons with isoprenoid side chains. Neftehimiâ 22, 723–788.

Pancost, R.D., Crawford, N., Maxwell, J.R., 2002. Molecular evidence for basin-scale photic zone euxinia in the Permian Zechstein Sea. Chem. Geol. 188, 217–227.

Parrish, J.T., 1993. Climate of the supercontinent Pangaea. J. Geol. 101, 215–233.

Peters, K.E., Moldowan, J.M., 1993. The Biomarker Guide: Interpreting Molecular Fossils in Petroleum and Ancient Sediments. Prentice-Hall, New Jersey. 393 pp.

Quenstedt, F.A., 1843. Das Flözgebirge Württembergs mit besonderer Rücksicht auf den Jura Laupp, Tübingen. 558 pp.

Quenstedt, F.A., 1858. Der Jura Laupp, Tübingen. 842 pp.

Radke, M., Welte, D.H., Wilsch, H., 1980. Preparative hydrocarbon group type determination by automated medium pressure liquid chromatography. Anal. Chem. 52, 406–411.

Requejo, A.G., Allan, J., Creaney, S., Gray, N.R., Cole, K.S., 1992. Aryl isoprenoids and diaromatic carotenoids in paleozoic source rocks and oils from western Canada and Williston Basins. Org. Geochem. 19, 245–264.

Riegraf, W., 1985. Mikrofauna, Biostratigraphie und Fazies im Unteren Toarcium Südwestdeutschlands und Vergleiche mit benachbarten Gebieten. Tübinger Mikropaläontologische Mitteilungen, Tübingen 3, 1–232.

Röhl, H.-J., Schmid-Röhl, A., 2004. Lower Toarcian (Upper Liassic) black shales of the Central European Epicontinental Basin: a sequence stratigraphic case study from the SW German Posidonia Shale (Lower Toarcian). SEPM Spec. Publ. (in press).

Röhl, H.-J., Schmid-Röhl, A., Oschmann, W., Frimmel, A., Schwark, L., 2001. The Posidonia Shale (Lower Toarcian) of SW-Germany: an oxygen-depleted ecosystem controlled by sea level and palaeoclimate. Palaeogeogr. Palaeoclimatol. Palaeoecol. 165, 27–52.

Sælen, G., Tyson, R.V., Telnæs, N., Talbot, M.R., 2000. Contrasting watermass conditions during deposition of the Whitby Mudstone (Lower Jurassic) and Kimmeridge Clay (Upper Jurassic) formations, UK. Palaeogeogr. Palaeoclimatol. Palaeoecol. 3–4, 163–196.

Schaefle, J., Ludwig, B., Albrecht, P., Ourisson, G., 1977. Hydrocarbures aromatiques d'origine geologique: II. Nouveaux carotenoides aromatiques fossiles. Tetrahedron Lett. 411, 3673–3676.

Schmid-Röhl, A., Röhl, J., Oschmann, W., Frimmel, A., Schwark, L., 2002. Palaeoenvironmental reconstruction of Lower Toarcian epicontinental black shales (Posidonia Shale, SW-Germany): global versus regional control. Geobios 35, 13–20.

Schouten, S., van Kaam-Peters, H.M.E., Rijpstra, W.I.C., Schoell, M., Sinninghe Damsté, J.S., 2000. Effects of an oceanic anoxic event on the stable carbon isotopic composition of early Toarcian carbon. Am. J. Sci. 300, 1–22.

Schwark, L., Püttmann, W., 1990. Aromatic hydrocarbon composition of the Permian Kupferschiefer in the Lower Rhine Basin. NW Germany. Org. Geochem. 16, 749–761.

Schwark, L., Vliex, M., Schaeffer, P., 1998. Geochemical characterization of Malm Zeta laminated carbonates from the Franconian Alb, SW-Germany (II). Org. Geochem. 29, 921–952.

Seilacher, A., 1982. Ammonite shells as habitats in the Posidonia Shales of Holzmaden—floats or benthic islands? Neues Jahrbuch für Geologie und Paläontologie. Monatshefte, Stuttgart 2, 98–114.

Sinninghe Damsté, J.S., Schouten, S., van Duin, A.C.T., 2001. Isorenieratene derivatives in sediments: possible controls on their distribution. Geochim. Cosmochim. Acta 65, 1557–1571.

Sirevåg, R., Buchanan, B.B., Berry, J.A., Troughton, J.H., 1977. Mechanisms of CO_2 fixation in bacterial photosynthesis studied by the carbon isotope technique. Arch. Microbiol. 59, 912–914.

Summons, R.E., Powell, T.G., 1986. Chlorobiaceae in palaeozoic seas revealed by biological markers, isotopes and geology. Nature 319, 763–765.

Summons, R.E., Powell, T.G., 1987. Identification of aryl isoprenoids in source rocks and crude oils: biological markers for the green sulphur bacteria. Geochim. Cosmochim. Acta 51, 557–566.

ten Haven, H.L., de Leeuw, J.W., Sinninghe Damsté, J.S., Schenk, P.A., Palmer, S.E., Zumberg, J., 1988. Application of biological markers in the recognition of palaeohypersaline environments. In: Fleet, A.J., Kelts, K., Talbot, M.R. (Eds.), Lacustrine Petroleum Source Rocks. Geol. Soc. Spec. Publ., vol. 40. Blackwell, Oxford, pp. 123–130.

van Kaam-Peters, H.M.E., 1997. The depositional environment of Jurassic organic rich sedimentary rocks in NW Europe: a biomarker approach. Geologica Ultraiectina, Utrecht (248 pp.).

Yu, X., Pu, F., Philp, R.P., 1990. Novel biomarkers found in South Florida Basin. Org. Geochem. 15, 433–438.

Ziegler, P.A., 1982. Geological Atlas of Central and Western Europe. Shell International Petroleum, Maatschappij B.V., Amsterdam. 130 pp.

Ziegler, P.A., 1988. Pangaea break-up: Jurassic–Early Cretaceous opening of Central and North Atlantic and Western Tethys. Mem.-Am. Assoc. Pet. Geol. 43, 91–110.